Radiomics Model Based on Shear-Wave Elastography Can Predict the Axillary Lymph Node Status in Early-Stage Breast Cancer

Meng Jiang
Tongji Hospital of Tongji Medical College of Huazhong University of Science and Technology Department of Geriatrics
Chang-Li Li
Hubei University of Chinese Medicine
Rui-Xue Chen
wuchan hospital
Shi-Chu Tang
Xiangya Hospital Central South University
Xiao-Mao Luo
Kunming Medical College Fourth Affiliated Hospital
Zhi-Rui Chuan
Kunming Medical College Fourth Affiliated Hospital
Wen-Zhi Lv
julei technology
Xin-Wu Cui (cuixinwu@live.cn)
Tongji Hospital of Tongji Medical College of Huazhong University of Science and Technology
https://orcid.org/0000-0003-3890-6660
Christoph F. Dietrich
Hirslanden Klinik Hirslanden

Research article

Keywords: Breast cancer, Axillary lymph node metastasis, Radiomics, Nomogram

Posted Date: September 17th, 2020

DOI: https://doi.org/10.21203/rs.3.rs-75554/v1

Abstract

Background: Accurate prediction of axillary lymph node (ALN) involvement in early-stage breast cancer is important for determining appropriate axillary treatment and therefore avoiding unnecessary axillary surgery and complications. This study aimed to develop and validate an ultrasound radiomics nomogram for preoperative evaluation of the ALN burden.

Methods: Data of 303 patients from Wuhan Tongji Hospital (training cohort) and 130 cases from Hunan Provincial Tumour Hospital (external validation cohort) between Jun 2016 and May 2019 were enrolled. Radiomic features were extracted from shear-wave elastography (SWE) and corresponding B-mode ultrasound (BMUS) images. Then, the minimum redundancy maximum relevance (MRMR) and least absolute shrinkage and selection operator (LASSO) algorithm were used to select ALN status-related features and construct the SWE and BMUS radiomic signatures. Proportional odds ordinal logistic regression was performed using the radiomic signature together with clinical data, and an ordinal nomogram was subsequently developed. We evaluated the performance of the nomogram using C-index, calibration, and compared it with clinical model.

Results: Multivariate analysis indicated that SWE signature, US-reported LN status and molecular subtype were independent risk factors associated with ALN status. The radiomics nomogram based on these variables showed good calibration and discrimination in the training set (overall C-index: 0.842; 95%CI, 0.773–0.879) and the validation set (overall C-index: 0.822; 95%CI, 0.765–0.838). For discriminating between disease-free axilla (N0) and any axillary metastasis (N + (≥1)), it achieved C-index of 0.845 (95%CI, 0.777–0.914) for the training cohort and 0.817 (95%CI, 0.769–0.865) for the validation cohort. The tool could also discriminate between low (N + (1–2)) and heavy metastatic burden of ALN (N + (≥3)), with C-index of 0.827 (95%CI, 0.742–0.913) for the training cohort and 0.810 (95%CI, 0.755–0.864) for the validation cohort.

Conclusions: The presented radiomics nomogram shows favourable predictive ability for ALN staging in patients with early-stage breast cancer, which could provide incremental information for preoperative decision-making.

Background

Worldwide, breast cancer is the most commonly diagnosed malignance and it has become the second leading cause of cancer-related death in women [1]. Axillary lymph node (ALN) status is one of the strongest predictors of long-term survival in primary breast cancer [2]. Mastectomy plus ALN dissection (ALND) was once regarded as the standard surgical strategy. However, ALND is associated with serval complications, including lymphedema (up to 25% of women following surgery), infection, shoulder stiffness, and major vessel and nerve injury [3]. Sentinel lymph-node (SLN) refers to the first lymph node that straightly drain the primary cancer. SLN dissection (SLND) is now widely applied to detect ALN status, especially for patients with clinically negative node [4, 5]. SLND has fewer complications

compared with ALND, but the incidence of potentially serious allergic reaction due to blue dye [6], radiation and costs related to radiocolloid injection [7], could not be eliminated. Besides, SLN biopsy and intraoperative frozen section examination would increase the operating and anaesthetic time.

The American College of Surgeons Oncology Group Z0011 (ACOSOG Z0011) trial revealed that among women with clinical T1/T2 breast cancer, if there were 1 or 2 SLNs involved, the spared of an ALND would not lead to inferior overall and disease-free survival [4, 5]. Thus, the number of involved ALNs may have great impact on patients' long-term survival outcome. According to the number of positive metastatic ALNs, we can categorize the patients into three subgroups: disease-free axilla (N0), low metastatic burden of ALN ($N_+(1–2)$), and heavy metastatic burden of ALN ($N_+(\geq 3)$), which is important for determining the extent of axillary treatment [4, 8, 9]. There were studies demonstrating that about 43–65% of patients who had positive SLNs underwent unnecessary ALND because of no additional non-SLN metastasis was detected, leading to high axillary morbidity [10, 11]. If there was reliable none-invasive preoperative methods for predicting different ALN burden, then individualized and precise minimally invasive treatment could be achieved to reduce the unnecessary SLND or ALND [12].

Two-dimensional (2D) shear wave elastography (SWE) is an elastographic technique that integrates B-model ultrasound (BMUS) with a color-coded map to allow for better characterization of breast lesions [13], which showed promise in distinguishing malignant and benign breast tumour [14]. Previous studies revealed that stiffness of breast cancer was also a predictor of ALN status, for higher shear wave velocity of breast cancer was related to higher possibility of ALN metastasis [15, 16]. However, traditional SWE parameters can only capture limited characteristics of the heterogeneous tumour, the area under the receiver operating characteristic curves (AUCs) for predicting ALN metastasis were 0.585–0.719 [17], which is unsatisfactory for clinical application.

Radiomics is an emerging technique that converts medical images into high-throughput features, which is valuable for tumour phenotyping [18]. Nomogram that combined radiomic signature extracted from US or MRI and clinicopathological factors has shown potential on discriminating N0 and any axillary metastasis (N+) [19, 20]. However, the use of radiomics nomogram to discriminate disease-free axilla, low ALN burden and heavy ALN burden has yet to be reported.

To address this, we aimed to develop and validated an ordinal nomogram incorporating 2D SWE radiomic signature for evaluating ALN status in early stage breast cancer. We focused on preoperatively discriminate pathologic N0, $N_+(1–2)$, and $N_+(\geq 3)$, because an accurate ALN burden evaluation is the basis of individual axillary treatment.

Materials And Methods

Study population

This retrospective study (clinical trial ChiCTR1900027676) was approved by the Institutional Review Board of the participant hospitals, and informed consent was waived. Between June 2016 and May 2019,

consecutive patients with primary breast cancer in hospital #1 (Tongji Hospital of Huazhong University of Science and Technology, training cohort) and hospital #2 (Hunan Provincial Tumour Hospital, validation cohort) referred for 2D SWE examination with subsequent biopsy and surgical treatment were evaluated.

Patient's inclusion criteria including: (1) pathologically confirmed primary breast cancer; (2) all patients underwent mastectomy with SLND or ALND (in case SLN biopsy was positive); (3) SWE image of breast displayed with the same BMUS image in split-screen mode was carried out within two weeks prior to operation; and (4) availability of clinical data. The exclusion criteria including: (1) preoperative therapy (neoadjuvant radiotherapy or chemotherapy) before US examination; (2) with multifocal lesions or bilateral disease; (3) little or no shear wave signal was obtained in the region of interest (ROI) of SWE (masses deeper than 3 cm in depth will lead to the attenuation of SWE); (4) missing important histopathological results, such as immunohistochemical (IHC) results or post-operative pathological ALN status. In total, 303 patients from Tongji Hospital comprised the training cohort (age, 51.11 ± 10.70 years; range, 27–85 years) were enrolled from Jun 2016 to April 2019. From March 2017 to May 2019, an independent external validation cohort of 130 patients (age, 50.98 ± 10.06 years; range, 33–82 years) from Hunan Provincial Tumour Hospital was enrolled with the same criteria. A flowchart describing the patient screening process is shown in **Figure 1**.

The US-reported LN status was obtained from the US reports, and axillary images containing important features of suspicious LNs were documented into the Picture Archiving and Communication Systems (PACS). It was retrospectively reviewed and verified by two radiologists (X.M.L and S.C.T, with 15 and 31 years of experience respectively). US features of LN used to assess suspicion for malignancy were as follows: 1) irregular cortical thickness ≥3 mm; 2) longest/shortest axes ratio < 2; or 3) absence of fatty hilum [21].

The baseline clinicopathological data were derived from the patient medical records, including age, clinical tumour size, pathological type, IHC results and post-operative ALN status. According to the 2017 St Gallen International Expert Consensus, the breast cancers were classified into four molecular subtypes based on preoperative biopsy: human epidermal growth factor receptor-2 positive (HER2+), triple-negative, Luminal A, and Luminal B [22]. The status of HER2, progesterone receptor (PR), estrogenic receptor (ER) and Ki-67 was assessed by IHC examination.

US image acquisition

BMUS and SWE examinations were performed with a Supersonic Aixplorer system (SuperSonic Imagine, Aix-en-Provence, France) using a 4-14 MHz linear transducer by five radiologists from Tongji Hospital and two radiologists from Hunan Tumour Hospital experienced in breast US according to standard protocols. After standard conventional BMUS, SWE was performed. The ROI was set to include the whole breast cancer and adjacent normal parenchyma for SWE acquisition, and stiffness was shown as a colour map on the ROI. On the colour map, blue and red regions reflect comparatively soft (low kPa) and stiff (high kPa) tissues, respectively [23]. The detail US examination procedures are presented in **Additional file 1**.

Tumour segmentation and radiomic feature extraction

Figure 2 shows the flowchart of the radiomics workflow. One image per tumour was used for analysis. The ROI for feature extraction was manually delineated on the largest cross section of B-model image using ITK-SNAP software (3.8.0; http://www.itksnap.org). All the manual segmentations were performed by two experienced breast US radiologists (with 11 and 9 years of experience, respectively) and each twice who were blinded from the final pathological diagnosis (for interobserver and intraobserver reproducibility evaluation). Because the contour of the lesion on SWE was indefinite, the same region on BMUS was copied and pasted to the corresponding SWE image, and was expanded to include the "stiff rim" sign if it existed. SWE is a combination of B-model image and pseudocolor elasticity layer, algorithms presented in previous studies were employed to produce clean quantitative images that mapping the tissue stiffness as grey levels [24-26]. The radiomic features were extracted automatically from each BMUS and SWE image by Pyradiomics (https://pyradiomics.readthedocs.io/en/latest/index.html) (**Additional file 2, Supplemental Table 1-6**) [27]. The stable features with interclass correlation coefficient (ICC) > 0.8 were selected to adapt different segmentations.

Radiomic signature building

We used Spearman's correlation coefficient to evaluate the relevance and redundancy of the features, and eliminated redundant features that with a Spearman's correlation coefficient ≥ 0.8. Then, the minimum redundancy maximum relevance (MRMR) algorithm and least absolute shrinkage and selection operator (LASSO) regression method using 10-fold cross-validation was applied to select the most useful predictive ALN status-related features from the training data set [28]. The formulas for the SWE and BMUS radiomic signatures were built using the respective selected features.

Radiomics nomogram construction

Univariate analysis was conducted to select statistically significant clinical factors associated with ALN metastasis. We mainly considered SWE radiomic signature in our nomogram; however, the incremental predictive value of BMUS radiomic signature to the model was also investigated using the net reclassification index (NRI) and integrated discriminatory improvement (IDI). Proportional odds ordinal logistic regression was used to build the radiomics nomogram based on the radiomic signatures and clinical characteristics [29]. The total points (Nomo-score) of each patients were calculated based on predictors of the nomogram. The association of the Nomo-score with pathologic ALN status was assessed using Spearman's correlation analysis. In addition, a classification procedure was proposed based on cut-offs of the Nomo-score to split patients into three subgroups of ALN status. Furthermore, a model based on clinical characteristics only was developed using the same method for comparison.

Performance evaluation

Harrell's C-indexes of the radiomics nomogram and clinical model were compared in the training and validation cohorts with Delong test. Besides, we carried out subgroup analysis based on patient age and clinical N stage, and calculated pairwise C-indexes for discriminating $N_+(\geq 1)$ versus N0, and $N_+(\geq 3)$ versus $N_+(1-2)$. The calibration curve was also plotted to measure the model. Among the subgroup analysis, $N_+(\geq 1)$ versus N0 is of special concern since it would determine the axillary surgical strategy. Decision curve analysis (DCA) was conducted accordingly to evaluate the clinical usefulness of the model in guiding SLN biopsy by quantifying the net benefits.

Statistical analysis

Statistical analyses were conducted with R software 3.6.1 and SPSS20.0 software (SPSS Inc., Chicago, IL). A two-sided *P* value less than 0.05 was used as the standard of statistically significant difference. In the univariate analysis, the differences in clinical characteristics between the patients of different groups were compared using Mann–Whitney U test or independent t test for continuous variables, and chi-square test or Fisher's exact test for categorical variables, as appropriate. Analysis of variance and Kruskal–Wallis H test were used for comparing more than two groups. The detailed descriptions of the LASSO and DCA algorithm are provided in the **Additional file 1**.

Results

Patient characteristics

The baseline characteristics of patients and postoperative pathological information of breast lesions in the training and validation cohorts are displayed in **Table 1** and **Table 2**. There were no significant differences between the two cohorts in age, clinical tumour size, status of hormone receptor (HR), HER2, ki67 and pathological type. According to the results of postoperative pathological analysis, 191 and 82 had disease-free axilla (N0), 46 and 26 had low ALN burden (N+(1–2)), 66 and 22 had heavy ALN burden (N+(≥3)) for the training and validation cohorts, respectively. There was no significant difference in ALN status between the two cohorts ($P = 0.312$). Of the total 433 patients, 262 (61%) had cT1 tumours and 171 (39%) had cT2 tumours. Among the 160 patients with ALN metastasis, 72 (45%) had one or two positive ALNs and 88 (55%) had three or more positive ALNs.

Feature selection and radiomics nomogram construction

Four-hundred two imaging features were extracted from each BMUS image. These features were reduced to six ALN status-related parameters after MRMR and LASSO algorithm in the training cohort (see **Additional file 3, Supplemental Figure 1 a-b**). Likewise, the 1558 SWE features were reduced to eight risk predictors by the same procedure (see **Additional file 3, Supplemental Figure 1 c-d**). Favourable interobserver and intraobserver reproducibility of feature extraction were achieved about these features, with intraobserver ICCs ranging from 0.803 to 0.891 and the interobserver ICCs ranging from 0.826 to 0.870. The BMUS and SWE radiomic signature calculation formulas are presented in the **Additional file 1**.

The multivariable regression analysis in the training cohort showed that SWE signature, molecular subtype and US-reported LN status were independent predictors for pathologic ALN status (**Table 3**). These predictors were combined into the radiomics nomogram (**Figure 3a**). The NRI and IDI analysis revealed that the addition of BMUS signature into the model did not show significantly better performance (NRI 0.0474, *P* = 0.130; IDI 0.0002, *P* = 0.861).

Model validation

As shown in **Figure 3b**, there was a significant positive correlation between Nomo-score and pathologic ALN status, which was also confirmed by Spearman's correlation coefficients (0.528 for training cohort and 0.580 for validation cohort, *P* < 0.001 for both, **Figure 3c**). As shown in **Table 4**, the radiomics nomogram achieved overall C-index of 0.842 (95% CI, 0.773-0.879) in the training cohort, and 0.822 (95% CI, 0.765-0.838) in the validation cohort. Besides, the model could well discriminate non-N0 from N0 groups (C-indexes: 0.845 for training and 0.817 for validation cohort), and discriminate N_+ (≥3) from N_+ (1–2) subgroup (C-indexes: 0.827 for training and 0.810 for validation cohort). Moreover, the radiomics model performed significantly better than the clinical model on both training and validation cohort (Delong test, P < 0.05).

The calibration curves showed good agreement between the nomogram predicted outcomes and the real ALN status (**Figure 4 a-b**). If we use this model to guide lymphadenectomy (non-N0 patients receive SLN biopsy and N0 patients do not), as shown in **Figure 4 c-d**, the decision curves show that the radiomic nomogram could add more benefit to patients than the clinical model, traditional axillary US examination, non-SLN biopsy scheme, and all-SLN biopsy scheme.

As shown in **Figure 5**, there was a trend from low to heavy ALN burden with increasing Nomo-score. For patients with a Nomo-score that ≤ 70, 96.67% (87/90, training cohort) and 100% (31/31, validation cohort) of the patients had less than three pathological metastatic ALNs. However, when the Nomo-score increased from 70 to 100, the percentage of N0 dropped from 90.00% (81/90) to 27.12% (16/59) for the training cohort, and dropped from 96.77% (30/31) to 14.81% (4/27) for the validation cohort. In patients with a Nomo-score of > 100, there was a percentage of 52.54% (31/59) and 48.15% (13/27) for heavy ALN burden in the training and validation cohort, respectively.

The stratified analysis showed that the performance of the radiomics nomogram was not affected by patient age, and was robust even in the US-reported LN negative subgroup (cN0) (**Additional file 3, Supplemental Figure 2**). Clinicians may be interested in how many patients with US-diagnosed N0 disease will be upstaged with the nomogram (non-N0 by pathology). These cases could be named as occult ALN metastasis, which are with no typical US signs. The results showed that the nomogram could well detect the patients with occult positive ALNs [82.1% (46/56) upgraded].

Discussion

In this study, we built an ordinal radiomics nomogram based on 2D SWE to predict the number of ALN metastases in breast cancer. The nomogram provided an easy-to-use and individualized tool for evaluating ALN status with high predictive ability, which can help tailor the optimum extent of axillary surgery.

Traditionally, regional ALNs with features of enlarged size, irregular shapes, unclear margins, or loss of fatty on US imaging are suspicious for nodal involvement, and these were usually applied to guide fine-needle aspiration biopsy [21]. However, this standard showed relatively poor performance in our cohorts, for several patients (56/160) who had pathologically positive ALNs have no suspicious nodal signs on US imaging. In contrast, our nomogram performed significantly better than the routinely used axillary US-guided ALN detection method. Moreover, 82.1% of the occult ALN metastasis with no typical US signs (missed by the radiologists) were detected by the nomogram, which demonstrated that our model could be an important supplement to the current US examination.

According to ACOSOG Z0011 results, early-stage breast cancer with less than three SLN metastases had no inferior long-tern survival if they received SLND only rather than ALND [4, 5]. Based on the findings, patients should undergo SLND first to clarify ALN status without considering whether they have clinically positive node or not [30]. However, SLND has false-negative rates ranging from 7.8–27.3%, which would lead to adverse outcomes including understaging the cancer and an increased risk of recurrence [31-33]. Our nomogram is able to distinguish patients with a negative ALN (N0) from those with any ALN status (N_+ ($\geq$1)), and performed better than the routine axillary US examination. For patients with Nomo-score of $\leq$70, the percentage of heavy ALN burden was only 3.33% and 0% for the training and validation cohort respectively. Thus, surgeons may potentially forgo other examinations or exploratory surgery to confirm the absence of positive non-SLN metastasis based on the SLND and can thereby avoid excessive treatments. Moreover, in patients with Nomo-score that >100, about half of the patients showed heavy ALN burden, this will increase the surgeon's confidence to perform ALND based on a positive SLN biopsy. Therefore, our nomogram showed the promise for assisting decision-making for appropriate axillary treatment based on the current retrievable clinical information. Surgeons can then consider various factors, including the calculated Nomo-score of individual patients, and other preoperative clinical information, as well as their own clinical experience, to make a comprehensive judgment on the proper surgery plan.

Compared with previous studies that using SWE values to predict ALN status [15, 17], our study obtained a better diagnostic performance by applying radiomic signature taken from the SWE images. Although the morphological and stiffness information of tumours can be easily discerned, high-dimensional radiomic features are still challenging to decipher through the naked eye (see **Additional file 3, Supplemental Figure 3**). Instead of measuring the breast cancer's stiffness based on the parameters of SWE, the whole shear wave ROI was quantified automatically into high throughput information and a large number of discriminative features could be acquired to phenotype the tumour. We further analysed the SWE radiomic features in the nomogram. Of note, the "wavelet-HL_gldm_DependenceNonUniformityNormalized_R" was the most significant radiomic feature of SWE in

primary cancer that correlated with the ALN status, which measures the similarity of dependence throughout the image, with a higher value indicating more heterogeneity of the tumour. The other seven SWE radiomic features also reflect the heterogeneity of the tumour in different aspects, implied that the higher the heterogeneity of the primary cancer are, and thus the higher possibility of tumoral invasiveness and heavy burden of ALN metastases is.

Next, we considered the clinicopathological characteristics. St Gallen molecular subtype, which show the pervasive differences of breast cancer in their gene expression patterns [34], was found to be significantly associated with ALN status in this study. Van Limbergen and colleagues pointed out that the HER2-enriched tumours were more likely to be lymph node positive [35]. Besides, Voduc and colleagues found that Luminal A tumours were associated with a lower risk of ALN metastasis than the other subtypes [36]. Our results have contributed to the accumulated evidence that molecular subtype could be a strong predictor of ALN status, and patients with positive HER2 were more inclined to ALN metastasis.

Our study has some unavoidable limitations. First, gene markers of breast cancer such as BRCA1 and BRCA2, are demonstrated helpful for patients risk stratification [37]. However, a radio-genomics analysis that focused on the combination of genomics and radiomic phenotypes, is not available currently based on the retrospective datasets. Second, patients with multifocal and bilateral breast disease were excluded since it is hard to determine which lesion would responsible for the metastatic ALN and should be input in the radiomics model. Finally, since it was a retrospective study, some of the axillary US examinations may not have purposefully identified all abnormal appearing LNs. In previous literature [9], ≥3 abnormal LNs on US was reported to be a strong predictor of heavy nodal burden. The contribution of the exact number of suspicious LN on US in the nomogram should be further investigated.

Conclusion

In conclusion, the radiomics nomogram had good predictive ability for ALN staging in early stage breast cancer, which could provide incremental information for individual diagnosis and treatment planning based on the current examination.

Abbreviations

ALN: axillary lymph node, BMUS: B-mode ultrasound, CI: confidence interval, HER2: human epidermal growth factor receptor 2, IHC: immunohistochemical, MRMR: minimum redundancy maximum relevance, ROC: receiver operating characteristic, SWE: shear-wave elastography, SLN: Sentinel lymph-node

Declarations

Ethics approval and consent to participate

This retrospective study (clinical trial ChiCTR1900027676) was approved by the Institutional Review Board of the participant hospitals, and informed consent was waived.

Consent for publication

Not applicable

Availability of data and materials

The datasets used and/or analysed during the current study are available from the corresponding author on reasonable request.

Competing interests

The authors declare that they have no competing interests.

Funding

This work was supported by the grant from Wuhan Science and Technology Bureau (No. 2017060201010181), Health Commission of Hubei Province (WJ2019M077, WJ2019H227) and Shihezi Science and Technology Bureau (2019ZH11), Key project supported by the Xinjiang Construction Corps (2019DB012). The funders did not have any role in this study design, data collection, data analysis, interpretation or writing of the manuscript.

Author contributions

M.J., C.L.L. and X.W.C. designed study. X.W.C. and S.C.T. provided the data of patients. M.J. and C.L.L. did literature search. M.J. and X.W.C. designed the figs. M.J., C.L.L., R.X.C., X.M.L., Z.R.C. and W.Z.L did data collection. M.J., X.W.C. and C.F.D did data analysis and interpretation. M.J. draft the manuscript, which was corrected and approved by all authors.

Acknowledgement

We thank all radiologists of the two study centres for their contributions to the study.

References

1. Siegel RL, Miller KD, Jemal A. Cancer statistics, 2020. CA: A Cancer Journal for Clinicians.2020; 70(1): 7-30.
2. Ahmed M, Purushotham AD, Douek M. Novel techniques for sentinel lymph node biopsy in breast cancer: a systematic review. Lancet Oncol. 2014; 15(8): e351-62.
3. Cardoso F, Kyriakides S, Ohno S, Penault-Llorca F, Poortmans P, Rubio IT, et al. Early breast cancer: ESMO Clinical Practice Guidelines for diagnosis, treatment and follow-up. Ann Oncol.2019; 30(8): 1194-220.
4. Giuliano AE, Ballman KV, McCall L, Beitsch PD, Brennan MB, Kelemen PR, et al. Effect of Axillary Dissection vs No Axillary Dissection on 10-Year Overall Survival Among Women With Invasive Breast

Cancer and Sentinel Node Metastasis. JAMA.2017; 318(10): 918.

5. Giuliano AE, Hunt KK, Ballman KV, Beitsch PD, Whitworth PW, Blumencranz PW, et al. Axillary dissection vs no axillary dissection in women with invasive breast cancer and sentinel node metastasis: a randomized clinical trial. JAMA.2011; 305(6): 569-75.
6. Bézu C, Coutant C, Salengro A, Daraï E, Rouzier R, Uzan S. Anaphylactic response to blue dye during sentinel lymph node biopsy. Surgical Oncology.2011; 20(1): e55-59.
7. Wang L, Yu J, Wang Y, Zuo W, Gao Y, Fan J, et al. Preoperative Lymphoscintigraphy Predicts the Successful Identification but Is Not Necessary in Sentinel Lymph Nodes Biopsy in Breast Cancer. Ann Surg Oncol.2007; 14(8): 2215-20.
8. Zheng X, Yao Z, Huang Y, Yu Y, Wang Y, Liu Y, et al. Deep learning radiomics can predict axillary lymph node status in early-stage breast cancer. Nat Commun.2020; 11(1): 1236.
9. Lim GH, Upadhyaya VS, Acosta HA, Lim JMA, Allen JC, Leong LCH. Preoperative predictors of high and low axillary nodal burden in Z0011 eligible breast cancer patients with a positive lymph node needle biopsy result. Eur J Surg Oncol. 2018; 44(7): 945-50.
10. Chu KU, Turner RR, Hansen NM, Brennan MB, Giuliano AE. Sentinel node metastasis in patients with breast carcinoma accurately predicts immunohistochemically detectable nonsentinel node metastasis. Ann Surg Oncol.1999; 6(8): 756-61.
11. Kamath VJ, Giuliano R, Dauway EL, Cantor A, Berman C, Ku NN, et al. Characteristics of the sentinel lymph node in breast cancer predict further involvement of higher-echelon nodes in the axilla: a study to evaluate the need for complete axillary lymph node dissection. Arch Surg.2001; 136(6): 688-92.
12. Kim GR, Choi JS, Han BK, Lee JE, Nam SJ, Ko EY, et al. Preoperative Axillary US in Early-Stage Breast Cancer: Potential to Prevent Unnecessary Axillary Lymph Node Dissection. Radiology.2018; 288(1): 55-63.
13. Youk JH, Kwak JY, Lee E, Son EJ, Kim JA. Grayscale Ultrasound Radiomic Features and Shear-Wave Elastography Radiomic Features in Benign and Malignant Breast Masses. Ultraschall Med.2020; 41(4):390-96.
14. Berg WA, Cosgrove DO, Doré CJ, Schäfer FK, Svensson WE, Hooley RJ, et al. Shear-wave elastography improves the specificity of breast US: the BE1 multinational study of 939 masses. Radiology.2012; 262(2): 435-49.
15. Evans A, Rauchhaus P, Whelehan P, Thomson K, Purdie CA, Jordan LB, et al. Does shear wave ultrasound independently predict axillary lymph node metastasis in women with invasive breast cancer? Breast Cancer Res Treat.2014; 143(1): 153-57.
16. Zhao Q, Sun JW, Zhou H, Du LY, Wang XL, Tao L, et al. Pre-operative Conventional Ultrasound and Sonoelastography Evaluation for Predicting Axillary Lymph Node Metastasis in Patients with Malignant Breast Lesions. Ultrasound Med Biol.2018; 44(12): 2587-95.
17. Youk JH, Son EJ, Kim JA, Gweon HM. Pre-Operative Evaluation of Axillary Lymph Node Status in Patients with Suspected Breast Cancer Using Shear Wave Elastography. Ultrasound Med Biol.2017; 43(8): 1581-86.

18. Bi WL, Hosny A, Schabath MB, Giger ML, Birkbak NJ, Mehrtash A, et al. Artificial intelligence in cancer imaging: Clinical challenges and applications. CA Cancer J Clin.2019; 69(2): 127-57.
19. Yu F, Wang J, Ye X, Deng J, Hang J, Yang B. Ultrasound-based radiomics nomogram: A potential biomarker to predict axillary lymph node metastasis in early-stage invasive breast cancer. Eur J Radiol.2019; 119:108658.
20. Han L, Zhu Y, Liu Z, Yu T, He C, Jiang W, et al. Radiomic nomogram for prediction of axillary lymph node metastasis in breast cancer. Eur Radiol.2019; 29(7): 3820-29.
21. Koelliker SL, Chung MA, Mainiero MB, Steinhoff MM, Cady B. Axillary lymph nodes: US-guided fine-needle aspiration for initial staging of breast cancer-correlation with primary tumor size. Radiology.2008; 246(1): 81-89.
22. Curigliano G, Burstein HJ, Winer EP, Gnant M, Dubsky P, Loibl S, et al. De-escalating and escalating treatments for early-stage breast cancer: the St. Gallen International Expert Consensus Conference on the Primary Therapy of Early Breast Cancer 2017. Ann Oncol.2017; 28(8): 1700-12.
23. Zhou J, Zhan W, Chang C, Zhang X, Jia Y, Dong Y, et al. Breast lesions: evaluation with shear wave elastography, with special emphasis on the "stiff rim" sign. Radiology.2014; 272(1): 63-72.
24. Li Y, Liu Y, Zhang M, Zhang G, Wang Z, Luo J. Radiomics With Attribute Bagging for Breast Tumor Classification Using Multimodal Ultrasound Images. J Ultrasound Med.2020; 39(2): 361-71.
25. Bhatia KS, Lam AC, Pang SW, Wang D, Ahuja AT. Feasibility Study of Texture Analysis Using Ultrasound Shear Wave Elastography to Predict Malignancy in Thyroid Nodules. Ultrasound Med Biol.2016; 42(7): 1671-80.
26. Jiang M, Li C, Tang S, Lv W, Yi A, Wang B, et al. Nomogram Based on Shear-Wave Elastography Radiomics Can Improve Preoperative Cervical Lymph Node Staging for Papillary Thyroid Carcinoma. Thyroid.2020; 30(6): 885-97.
27. van Griethuysen J, Fedorov A, Parmar C, Hosny A, Aucoin N, Narayan V, et al. Computational Radiomics System to Decode the Radiographic Phenotype. Cancer Res.2017; 77(21): e104-07.
28. Sauerbrei W, Royston P, Binder H. Selection of important variables and determination of functional form for continuous predictors in multivariable model building. Stat Med.2007; 26(30): 5512-28.
29. Harrell F. Regression Modeling Strategies. New York, NY: Springer;2001.
30. Farrell TPJ, Adams NC, Stenson M, Carroll PA, Griffin M, Connolly EM, et al. The Z0011 Trial: Is this the end of axillary ultrasound in the pre-operative assessment of breast cancer patients? Eur Radiol.2015; 25(9): 2682-87.
31. Krag D, Weaver D, Ashikaga T, Moffat F, Klimberg VS, Shriver C, et al. The sentinel node in breast cancer--a multicenter validation study. N Engl J Med.1998; 339(14): 941-46.
32. Krag DN, Anderson SJ, Julian TB, Brown AM, Harlow SP, Ashikaga T, et al. Technical outcomes of sentinel-lymph-node resection and conventional axillary-lymph-node dissection in patients with clinically node-negative breast cancer: results from the NSABP B-32 randomised phase III trial. Lancet Oncol.2007; 8(10): 881-88.

33. Pesek S, Ashikaga T, Krag LE, Krag D. The false-negative rate of sentinel node biopsy in patients with breast cancer: a meta-analysis. World J Surg.2012; 36(9): 2239-51.
34. Goldhirsch A, Winer EP, Coates AS, Gelber RD, Piccart-Gebhart M, Thürlimann B, et al. Personalizing the treatment of women with early breast cancer: highlights of the St Gallen International Expert Consensus on the Primary Therapy of Early Breast Cancer 2013. Ann Oncol.2013; 24(9): 2206-23.
35. Van Calster B, Vanden Bempt I, Drijkoningen M, Pochet N, Cheng J, Van Huffel S, et al. Axillary lymph node status of operable breast cancers by combined steroid receptor and HER-2 status: triple positive tumours are more likely lymph node positive. Breast Cancer Res Tr.2009; 113(1): 181-87.
36. Voduc KD, Cheang MCU, Tyldesley S, Gelmon K, Nielsen TO, Kennecke H. Breast Cancer Subtypes and the Risk of Local and Regional Relapse. J Clin Oncol.2010; 28(10): 1684-91.
37. Pinker K, Chin J, Melsaether AN, Morris EA, Moy L. Precision Medicine and Radiogenomics in Breast Cancer: New Approaches toward Diagnosis and Treatment. Radiology.2018; 287(3): 732-47.

Tables

Table 1 Clinical characteristics of patients in the training and validation cohorts

Characteristic	Training (n=303)	Validation (n=130)	*P* value
Age, mean ± SD, years	51.11 ± 10.70	50.98 ± 10.06	0.907
ALN metastasis (%)			0.312
N0	191 (63.0)	82 (63.1)	
N_+(1–2)	46 (15.2)	26 (20.0)	
N_+(≥3)	66 (21.8)	22 (16.9)	
Clinical tumour size (cm)	2.35 ± 1.16	2.49 ± 1.19	0.253
Clinical T stage (%)			0.293
cT1	190 (62.7)	72 (55.4)	
cT2	113 (37.3)	58 (44.6)	
US-reported LN status (%)			
Positive	114 (37.6)	56 (43.1)	0.287
Negative	189 (62.4)	74 (56.9)	
Histologic type (%)			
Ductal	259 (85.5)	116 (89.2)	0.483
Lobular or mixed	9 (3.0)	4 (3.1)	
Other	35 (11.6)	10 (7.7)	
Estrogenic receptor (%)			0.432
Positive	212 (70.0)	86 (66.2)	
Negaunee	91 (30.0)	44 (33.8)	
Progesterone receptor (%)			0.068
Positive	207 (68.3)	77 (59.2)	
Negaunee	96 (31.7)	53 (40.8)	
HER2 (%)			0.208
Positive	52 (17.2)	29 (22.3)	
Negaunee	251 (82.8)	101 (77.7)	
Ki-67 status (%)			0.102
Positive	226 (74.6)	87 (66.9)	
Negaunee	77 (25.4)	43 (33.1)	

Molecular subtype (%)			
Luminal A	64 (21.1)	29 (23.3)	0.431
Luminal B	159 (52.5)	60 (46.2)	
HER2 positive	33 (10.9)	13 (10.0)	
Basal-like	47 (15.5)	28 (21.5)	
BMUS signature, median (interquartile range)	0.62 (0.49 to 0.69)	0.64 (0.49 to 0.71)	0.414
SWE signature, median (interquartile range)	0.59 (0.50 to 0.72)	0.61 (0.47 to 0.72)	0.960

Abbreviations: US ultrasound, LN lymph node, BMUS B-model ultrasound, SWE shear-wave elastography.

Table 2 Pathological characteristics of the lesions after surgery

	Training cohort (n = 303)	Validation cohort (n = 130)
Histological grade		
I	30 (9.9)	12 (9.2)
II	160 (52.8)	77 (59.2)
III	113 (37.3)	41 (31.6)
Pathologic T stage, No. (%)		
pT1	105 (34.7)	63 (48.5)
pT2	183 (60.4)	60 (46.2)
pT3	15 (5.0)	7 (5.4)
Pathologic N stage, No. (%)		
pN0	191 (63.0)	82 (63.1)
pN1	67 (22.1)	26 (20.0)
pN2	30 (9.9)	14 (10.8)
pN3	15 (5.0)	8 (6.2)
Number of LNs removed		
Median	14	14
Mean	12	13
Interquartile range	5-17	6-17
Number of positive LNs		
Median	0	0
Mean	2	2
Interquartile range	0-2	0-1

Abbreviations: LNs lymph nodes.

Table 3 Construction of radiomics nomogram and clinical model via multivariable ordinal logistic regression analysis

		Clinical model			Radiomics nomogram	
Intercept and variable	**Coef**	**Effect (95% CI)**	***P* value**	**Coef**	**Effect (95% CI)**	***P* value**
Intercept 1	-1.693	NA	<0.001	-6.547	NA	<0.001
Intercept 2	-2.578	NA	<0.001	-7.626	NA	<0.001
Molecular subtype						
Luminal A	Ref			Ref		
Luminal B	0.843	0.431 (0.215–0.863)	0.018	0.450	0.637 (0.297–1.368)	0.248
HER2+	-1.046	0.151 (0.053–0.434)	0.084	-2.305	0.064 (0.020–0.201)	0.0006
Basal-like	0.546	0.743 (0.384–1.436)	0.209	-0.334	0.457 (0.221–0.941)	0.487
US-reported LN status	1.605	4.979 (3.010–8.236)	<0.001	2.034	7.648 (4.288–13.640)	<0.001
SWE signature	NA	NA	NA	8.490	6.543 (3.880–11.034)	<0.001

Abbreviations: US ultrasound, SWE shear-wave elastography, LNs lymph nodes, NA not available.

Table 4 Performances of the radiomics nomogram in the training and validation cohorts

	Variables	Clinical model	Radiomics nomogram	******P* value
Overall C-index	Training cohort	0.712 (0.613–0.760)	0.842 (0.773–0.879)	<0.001
	Validation cohort	0.764 (0.694–0.812)	0.822 (0.765–0.838)	<0.001
Pairwise C-index	$N_+(\geq 1)$ vs N0			
	Training cohort	0.767 (0.682–0.852)	0.845 (0.777–0.914)	<0.001
	Validation cohort	0.676 (0.613–0.739)	0.817 (0.769–0.865)	<0.001
	$N_+(\geq 3)$ vs $N_+(1–2)$			
	Training cohort	0.750 (0.651–0.849)	0.827 (0.742–0.913)	0.013
	Validation cohort	0.663 (0.588–0.739)	0.810 (0.755–0.864)	0.039

Data in parentheses are 95% confidence intervals.

*P value represents difference of C-index between the radiomics nomogram and clinical model.

Figures

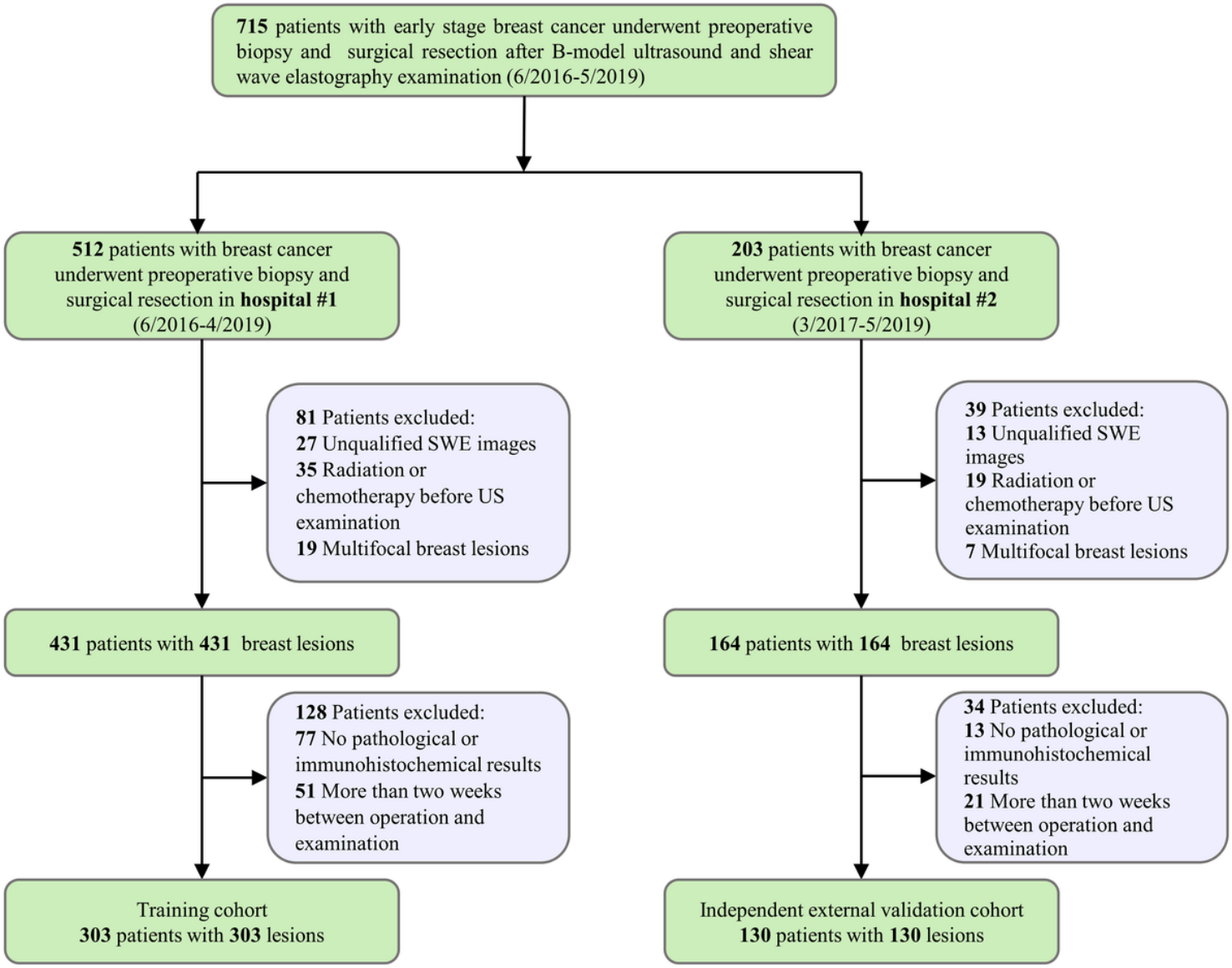

Figure 1

Flowchart shows inclusion and exclusion criteria.

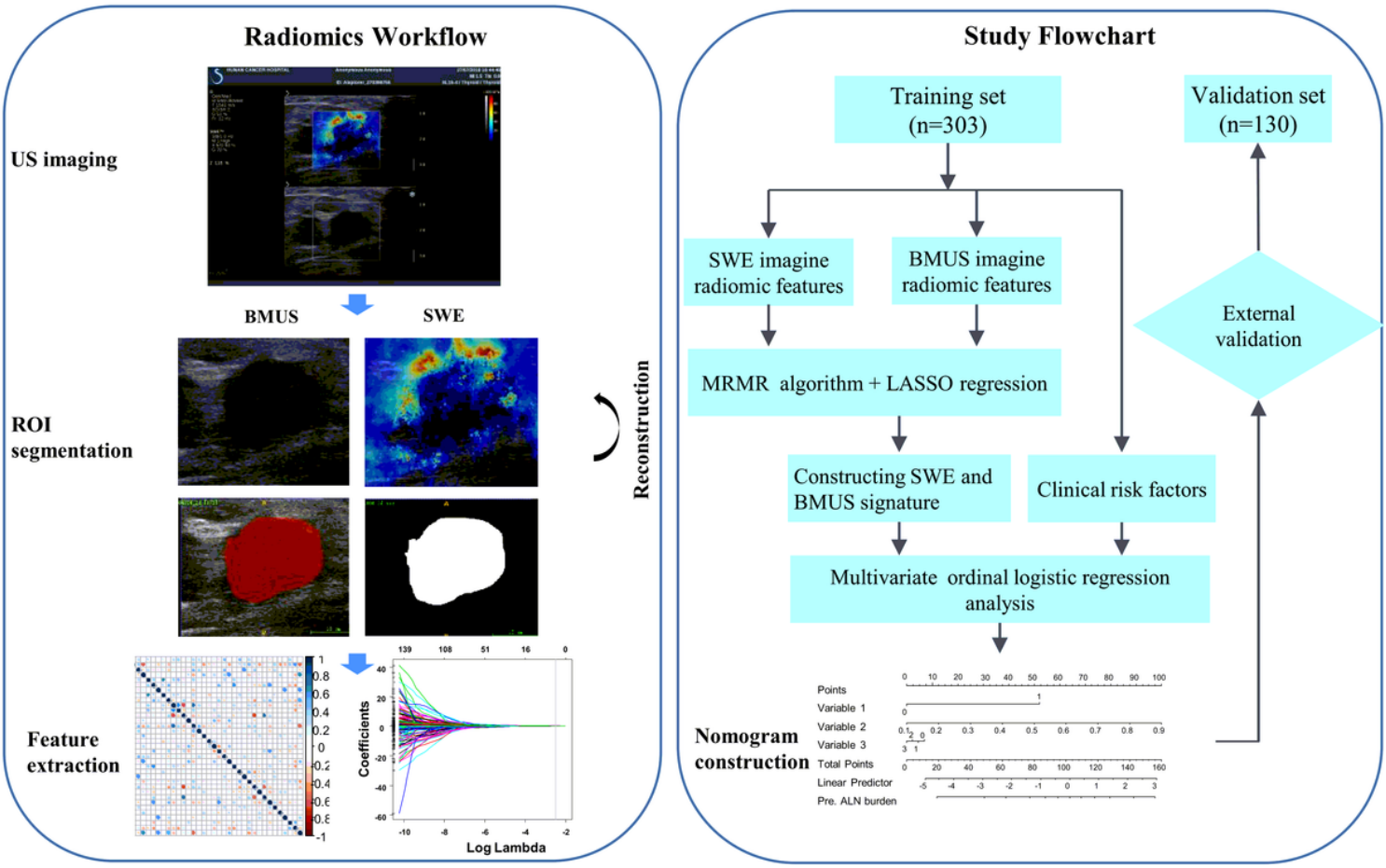

Figure 2

Ultrasound radiomics workflow and study flowchart. Abbreviations: ROI region of interest, BMUS B-model ultrasound, SWE shear-wave elastography, MRMR minimum redundancy maximum relevance, SVM support vector machine.

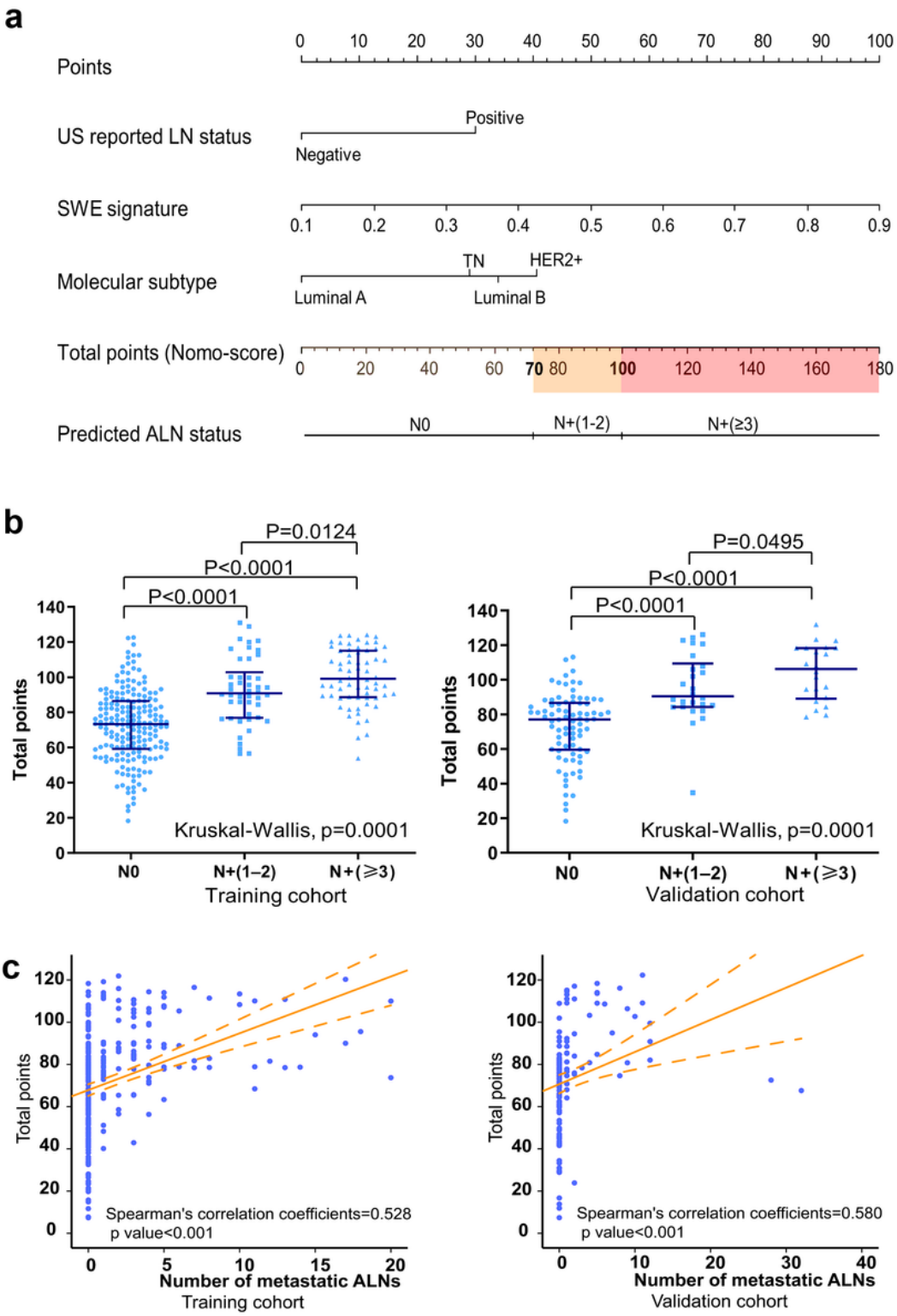

Figure 3

The radiomics nomogram and its performance. (a) Nomogram with SWE radiomic signature, molecular subtype and US-reported LN status. The points of each predictor are obtained based on the top 'points' bar with scale of 0 to 100. Then, the total point is calculated by summing the three points. The predicted ALN status is obtained by mapping the total point to the 'total points' bar and the 'predicted ALN status' bar. (b) Scatter diagram showing patterns of correlation between ALN status and Nomo-score in the

training and validation cohorts. (c) The correlation between the number of metastatic ALNs and Nomo-score.

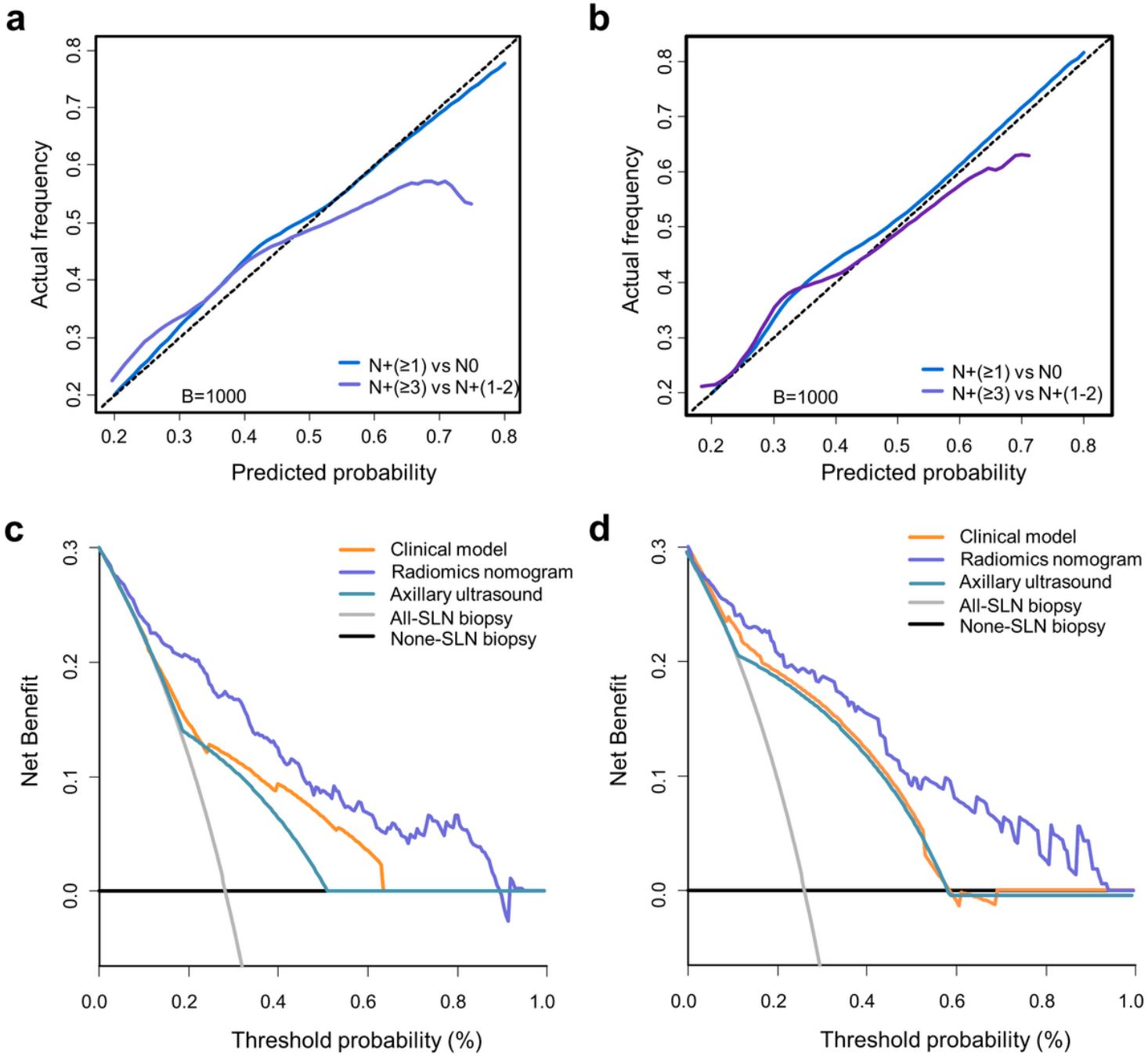

Figure 4

The calibration curve (training set: a; validation set: b) and decision curve (training set: c; validation set: d) of the nomogram.

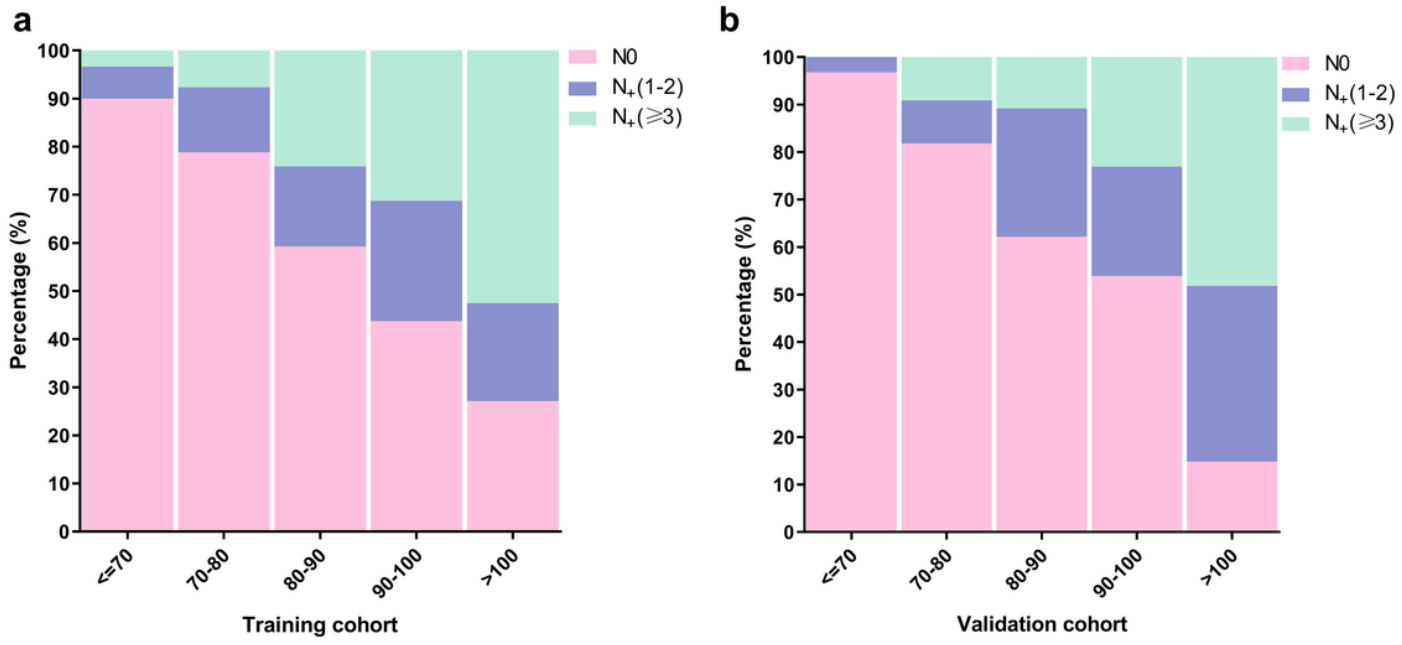

Figure 5

Bar graphs represent the percentage of patient to develop disease-free axilla (N0), low ALN burden (N+(1–2)), and heavy ALN burden (N+(≥ 3)) based on the cut-off values of the Nomo-score.

Supplementary Files

This is a list of supplementary files associated with this preprint. Click to download.

- ADDITIONALFILE3.docx
- ADDITIONALFILE2.docx
- ADDITIONALFILE1.docx